

Small-Molecule-Induced Clustering of Heparan Sulfate Promotes Cell Adhesion

Naohiro Takemoto,^{†,‡} Tetsuya Suehara,[§] Heidie L. Frisco,^{†,‡} Shin-ichi Sato,[†] Takuhito Sezaki,[⊥] Kosuke Kusamori,[§] Yoshinori Kawazoe,[‡] Sun Min Park,[†] Sayumi Yamazoe,^{†,‡} Yoshiyuki Mizuhata,[‡] Rintaro Inoue,[‡] Gavin J. Miller,[#] Steen U. Hansen,[#] Gordon C. Jayson,^{||,#} John M. Gardiner,[#] Toshiji Kanaya,[‡] Norihiro Tokitoh,[‡] Kazumitsu Ueda,[⊥] Yoshinobu Takakura,[§] Noriyuki Kioka,[⊥] Makiya Nishikawa,^{*,§} and Motonari Uesugi^{*,†,‡}

[†]Institute for Integrated Cell-Material Sciences (WPI-iCeMS) and [‡]Institute for Chemical Research, Kyoto University, Uji, Kyoto 611-0011, Japan

[§]Graduate School of Pharmaceutical Sciences, Kyoto University, Kyoto, Kyoto 606-8501, Japan

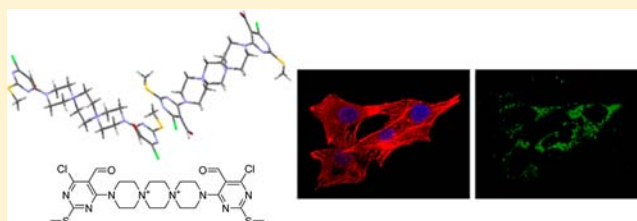
[⊥]Graduate School of Agriculture, Kyoto University, Kyoto, Kyoto 606-8502, Japan

^{||}School of Cancer and Enabling Sciences, University of Manchester, Manchester M20 4BX, U.K.

[#]Manchester Institute of Biotechnology, School of Chemistry, Faculty of EPS, University of Manchester, Manchester M1 7DN, U.K.

Supporting Information

ABSTRACT: Adhesamine is an organic small molecule that promotes adhesion and growth of cultured human cells by binding selectively to heparan sulfate on the cell surface. The present study combined chemical, physicochemical, and cell biological experiments, using adhesamine and its analogues, to examine the mechanism by which this dumbbell-shaped, non-peptidic molecule induces physiologically relevant cell adhesion. The results suggest that multiple adhesamine molecules cooperatively bind to heparan sulfate and induce its assembly, promoting clustering of heparan sulfate-bound syndecan-4 on the cell surface. A pilot study showed that adhesamine improved the viability and attachment of transplanted cells in mice. Further studies of adhesamine and other small molecules could lead to the design of assembly-inducing molecules for use in cell biology and cell therapy.



INTRODUCTION

Adhesamine (1) has been discovered by cell-based screening of an in-house chemical library as a small molecule that promotes adhesion and growth of cultured human cells.¹ Adhesamine has been demonstrated to promote normal, physiologically relevant cell adhesion: the cell adhesion induced by adhesamine is accompanied by phosphorylation of focal adhesion kinase (FAK) and extracellular signal-related kinase (ERK), actin reorganization, and focal adhesion formation. The unique structure of this dumbbell-shaped molecule may provide a basis for the design of completely defined, synthetic organic molecules that are useful for biological and medical applications.^{1,2}

Results of previous chemical, biochemical, and cell biological analyses suggested that the molecular target of adhesamine is heparan sulfate on the cell surface.¹ A number of heparan sulfate-binding molecules have been reported in addition to adhesamine.³ However, to our knowledge, only peptidic molecules have previously been shown to enhance cell adhesion through “agonistic” activities; adhesamine appears to be the first non-peptidic small organic molecule that promotes physiological cell adhesion. It has remained unknown how this organic

small molecule promotes cell adhesion and growth by binding selectively to heparan sulfate. The present study reports an attempted elucidation of the molecular mechanism of the small-molecule-induced physiological cell adhesion.

RESULTS AND DISCUSSION

Structure–Activity Relationship. Previous structure–activity relationship studies¹ indicated that both the aromatic and dispirotriperazine moieties are essential and that the aldehyde groups can be reduced or changed without affecting the biological activity. It was also suggested that the positively charged nitrogen atoms in the central segment (Figure 1) are important but not sufficient for the interaction with negatively charged heparan sulfate; an adhesamine analogue with no positive charge or the dispirotriperazine alone exhibit no detectable biological activity. The shape of the positively charged dispirotriperazine skeleton appeared to be critical. To examine the conformation of the dispirotriperazine moiety, we conducted X-ray crystallographic analysis of adhesamine

Received: February 21, 2013

Published: July 3, 2013

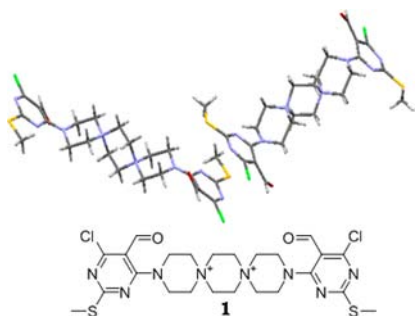


Figure 1. X-ray crystal structure of adhesamine (**1**). Counteranions (TFA) and water molecules are omitted for clarity. CCDC: 850155.

(Figure 1). In the crystal structure, each of the three piperazine rings adopts a chair conformation, oriented perpendicular to one another, and the dispirotripiperazine moiety displays an overall linear structure.

To determine the mechanistic role of the dispirotripiperazine segment, we chemically synthesized and biologically evaluated adhesamine analogues in which that segment was modified (Figure 2). The cell adhesion activities of the analogues were

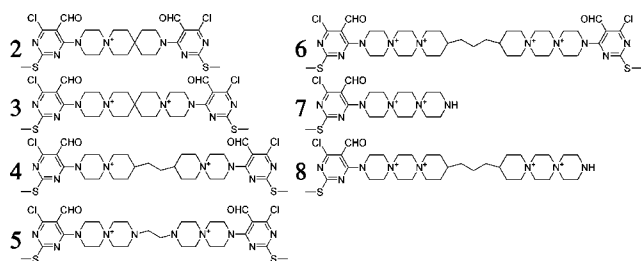


Figure 2. Chemical structures of adhesamine analogues. Counteranions (TFA) are omitted for clarity.

measured using Jurkat cells, which are floating human lymphoma cells. Isothermal titration calorimetry (ITC) was employed to estimate the affinity of the analogues to heparin oligosaccharides, simple models of heparan sulfate. These purified, fractionated oligomers are made from heparin by controlled deaminative cleavage. Although their electrophoretic mobilities on a polyacrylamide gel were consistent with their lengths (Supporting Information Figure S1), their structures are not completely defined. Thus, experimental thermodynamic data were treated as apparent values.

Molecule **2**, an adhesamine analogue in which a positively charged nitrogen atom was replaced by a carbon atom, failed to bind to heparin decasaccharide under the test conditions, generating no detectable ΔH (the change in enthalpy) value, and exhibited no detectable effect on cell attachment (Supporting Information Figures S2 and S3a). These results suggest that the two positively charged nitrogen atoms are essential for adhesamine to be effective.

Molecules **3–5**, in which the distance between the two important nitrogen atoms was extended, also failed to bind to heparin decasaccharide or affect cell adhesion (Supporting Information Figures S2 and S3b-d). These results suggest that the two positively charged nitrogen atoms need to be in close proximity for the molecule to bind to heparin and exhibit biological activity.

Cooperative Association of Adhesamine with Heparin. While evaluating the affinity of adhesamine for heparin

oligosaccharides with different lengths (hexa, octa, and deca) using ITC, we noted an interesting trend: ΔH and ΔG (Gibbs's free energy) values were dependent on the length of the heparin oligosaccharide. The experiment with hexasaccharide generated no ΔH value under the test conditions, while experiments with octasaccharide and decasaccharide resulted in apparent ΔH values of -3.9 and -8.3 kcal/mol of adhesamine, and apparent ΔG values of -7.4 and -7.7 kcal/mol, respectively. The numbers of bound adhesamine molecules and the entropy loss of the binding were also related to the length of the oligosaccharide: 4.48 molecules for an octasaccharide and 6.41 molecules for a decasaccharide; apparent ΔS (the change in entropy) values were 11.7 cal/mol-deg for octasaccharide and -2.11 cal/mol-deg for decasaccharide (Table 1 and Supporting Information Figure

Table 1. Thermodynamic Values for the Interaction of Adhesamine (1**) or Conjugate **6** with Heparin Oligosaccharides^a**

heparin oligosaccharide	^{app} ΔH (kcal/mol)	^{app} ΔG (kcal/mol)	^{app} ΔS (cal/mol-deg)	^{app} n^b
1 + hexasaccharide	nd	nd	nd	nd
1 + octasaccharide	-3.94	-7.43	11.7	4.48
1 + decasaccharide	-8.34	-7.71	-2.11	6.41
6 + tetrasaccharide	nd	nd	nd	nd
6 + hexasaccharide	-8.02	-7.85	-0.56	1.98
6 + octasaccharide	-11.56	-7.84	-12.5	2.19
6 + decasaccharide	-16.78	-8.20	-28.8	2.99

^aAll data were collected in 50 mM sodium phosphate buffer (pH 6.0) containing 10 mM NaCl and 2% (v/v) DMSO at 25 °C. nd = not detectable. app = apparent values. ^bNumber of molecules of **1** or **6** per oligosaccharide.

S4). Such thermodynamic characteristics are often observed in a cooperative interaction of multiple ligands with a receptor, including DNA–protein interactions,⁴ suggesting that the interaction of adhesamine with heparin is not a collection of independent 1:1 complexations.

Design and Evaluation of Dimer-like Molecule **6.** Close examination of the X-ray crystal structure of adhesamine revealed that two adhesamine molecules interact with each other through parallel displaced π – π stacking of pyrimidine rings (Figure 1). Although there was a possibility that the stacking interaction was due to crystal packing, we hypothesized that a similar self-association of adhesamine might take place upon cooperative binding to heparan sulfate in solution.

The hypothesis was tested by synthesizing a dimer-like molecule (**6**), in which two molecules of adhesamine were covalently conjugated by replacing two pyrimidine rings with an alkyl linker (Figure 2). Our prediction was that conjugate **6** would be biologically active and behave just like a dimer in ITC experiments.

As predicted, conjugate **6** promoted cell adhesion at essentially the same levels as adhesamine (Supporting Information Figure S5). ITC measurements for conjugate **6** gave apparent ΔH values of -8.0 , -11.6 , and -16.8 kcal/mol, respectively, for hexa-, octa-, and decasaccharides, which are

approximately twice the values for adhesamine (Table 1 and Supporting Information Figure S6). ΔH values of conjugate **6** were dependent on the length of the heparin oligosaccharide, suggesting a cooperative interaction. ITC results showed that 1.98 conjugate **6** molecules were associated with a heparin hexasaccharide, 2.19 molecules with an octasaccharide, and 2.99 with a decasaccharide. These numbers are approximately half those obtained for adhesamine, supporting our hypothesis that conjugate **6** mimics a dimer of adhesamine. It is interesting to note that the sample of octasaccharide showed a ΔH value larger than that of hexasaccharide, but smaller than that of decasaccharide. The intermediate ΔH value might be due to the intermediate size of the octasaccharide, which is long enough to accommodate two molecules of conjugate **6**, but not three. The observed ΔH value could reflect a mixture of 1:2 and incomplete 1:3 complexes.

These thermodynamic data are mostly consistent with our model of cooperative association of adhesamine. However, detailed examination of the data pointed out two intriguing properties. One is the inability of conjugate **6** to exhibit detectable ΔH values with a tetrasaccharide, or adhesamine with a hexasaccharide. The observation that 1.98 or 2.99 molecules of conjugate **6** bind to hexa- or decasaccharide, respectively, suggests that one molecule of conjugate **6** requires at least a trisaccharide for its interaction. Similarly, the observation that 4.48 or 6.41 molecules of adhesamine bind to octa- or decasaccharide, respectively, suggests that two molecules of adhesamine require a host saccharide slightly longer than a trisaccharide. Although this estimation leads to the assumption that one molecule of conjugate **6** binds to a tetrasaccharide, or that 3–4 molecules of adhesamine bind to a hexasaccharide, we failed to detect their ΔH values. One likely explanation would be that the cooperative interaction of these molecules was insufficient to generate detectable ΔH under the experimental conditions. In a cooperative interaction, multiple ligands potentiate their affinity to a macromolecular target by interacting with each other. Cooperative association of more than two molecules of conjugate **6**, or more than 4–5 molecules of adhesamine might be necessary for detectable affinity.

Another point to note is that adhesamine has a more favorable ΔS value than conjugate **6**. Linking two independent ligands usually results in a ΔS more favorable for the interaction, because when linked ligands bind, the entropy cost of restricting ligand rotation and translation only needs to be paid once.⁵ The more favorable ΔS values we observed for adhesamine might be due to a number of other factors that influence the amount of entropy in a system. One possibility is entropy–enthalpy compensation, in which binding that is tighter or more favorable in terms of enthalpy results in greater entropic restriction.⁶ The covalent linkage of conjugate **6** might restrict the conformational flexibility of its entire complex, which would have an unfavorable effects on entropy. Another possibility is preorganization of ligands where ligands are conformationally prepared and desolvated, prior to their interaction with the host. As observed in the crystal structure, multiple adhesamine molecules might already have been self-assembled and desolvated to some degree without a heparin saccharide in solution, reducing the beneficial entropic effects of connecting two ligands with a relatively flexible alkyl linker. The unusual ΔS values observed for conjugate **6** are likely to arise from complex interplays of various factors, and particular care needs to be taken in their interpretation. Nevertheless these

thermodynamic data are consistent overall with the cooperative association model. Further studies including structural analysis are needed to confirm the model.

CD titration experiments⁷ were performed to compare the interactions of heparin with adhesamine and conjugate **6** (Supporting Information Figure S7). Adhesamine alone exhibited no CD signals; however, addition of heparin induced negative and positive Cotton effects at 326 and 271 nm, respectively, which are close to the absorption wavelengths of adhesamine. Similar Cotton effects were observed when heparin was added to conjugate **6**, suggesting that conjugate **6** and adhesamine bind to heparin in an analogous manner. These results provide further support for our hypothesis that conjugate **6** mimics a dimer of adhesamine.

Design and Evaluation of Molecules 7 and 8. To further test the cooperative-binding hypothesis, we synthesized and evaluated molecule **7** and conjugate **8**, which lacked one of the two pyrimidine rings of adhesamine (**1**) or conjugate **6**, respectively (Figure 2). If our hypothesis is correct, molecules **7** and **8** would exhibit less affinity to heparin due to reduced cooperativity. The lack of a pyrimidine ring at one end would allow conjugates **7** and **8** to form a dimer, but not oligomers, upon binding to an oligosaccharide, independent of the length of oligosaccharide.

ITC analysis showed that molecule **7** generated no detectable ΔH value when mixed with heparin polymer (Figure 3 and

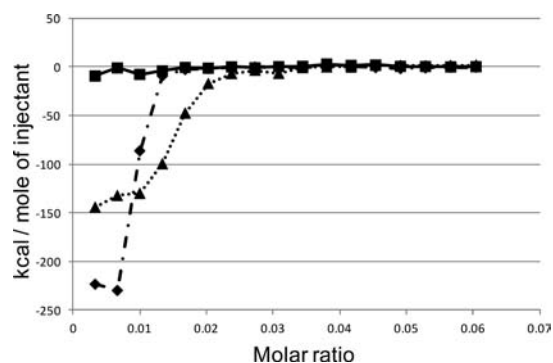


Figure 3. Inhibitory effects of molecule **7** on the interaction between adhesamine and heparin. ITC experiments are performed for monitoring the adhesamine-heparin interactions in the presence or absence of molecule **7**. The concentration of heparin was 50 μM . Integrated heat data are shown. Individual tracings are (■) **7** (150 μM), (◆) adhesamine (150 μM), and (▲) a mixture of adhesamine (150 μM) and **7** (150 μM). All data were collected in 50 mM sodium phosphate buffer (pH 6.0) containing 10 mM NaCl and 2% (v/v) DMSO at 25 °C.

Supporting Information Figure S8), perhaps due to its inability to undergo pyrimidine-mediated oligomerization. When molecule **7** was doped into a sample of adhesamine, the binding of adhesamine to heparin polymer decreased, possibly because molecule **7** terminates the cooperativity (Figure 3). On the other hand, conjugate **8** exhibited similar ΔH and ΔG values for different oligosaccharides: apparent $\Delta H = -4.4$, -3.3 , and -4.8 kcal/mol, and apparent $\Delta G = -6.90$, -7.00 , and -7.00 kcal/mol for hexa-, octa-, and decasaccharides, respectively (Table 2 and Supporting Information Figure S9). The numbers of conjugate **8** molecules that were associated with a heparin oligosaccharide were also close to each other: 2.32, 2.07, and 2.34 molecules for hexa-, octa-, and decasaccharides, respectively. Overall, these results support

Table 2. Thermodynamic Values for the Interaction of Conjugate 8 with Heparin Oligosaccharides^a

heparin oligosaccharide	^{app} ΔH (kcal/mol)	^{app} ΔG (kcal/mol)	^{app} ΔS (cal/mol-deg)	^{app} n^b
hexasaccharide	-4.41	-6.90	8.34	2.32
octasaccharide	-3.28	-7.00	12.5	2.07
decasaccharide	-4.76	-7.00	7.53	2.34

^aAll data were collected in 50 mM sodium phosphate buffer (pH 6.0) containing 10 mM NaCl and 2% (v/v) DMSO at 25 °C. ^bNumber of molecules of 8 per oligosaccharide.

the hypothesis that multiple adhesamine molecules cooperatively bind to heparin through oligomerization induced by pyrimidine–pyrimidine interactions.

Although the stoichiometries (n) of conjugates 6 and 8 for hexasaccharides are close, the ΔH values of these conjugates are significantly different. One possible explanation would be participation of the pyrimidine moiety in the association with heparin oligosaccharides in addition to its role in mediating oligomerization. Further studies are needed to clarify the exact roles of the pyrimidine moiety.

Comparison with Synthetic Heparin Oligomers. In the ITC experiments described above, we used purified oligomers made from naturally occurring heparin. These fractionated oligomers consist of variably sulfated, heterogeneous saccharides: glucuronic acid (GlcA) or iduronic acid (IdoA) and glucosamine (GlcN). For a comparison, we prepared two structurally defined heparin oligomers: octasaccharide (GlcNS6S-IdoA2S)₄-OMe and decasaccharide (GlcNS6S-IdoA2S)₅-OMe (Figure 4). These fully sulfated versions of

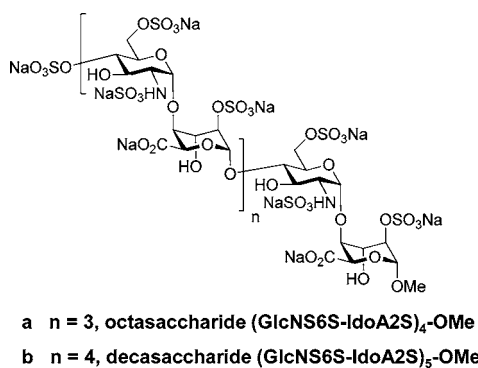


Figure 4. Chemical structures of synthetic heparin oligosaccharides: (a) synthetic octasaccharide (GlcNS6S-IdoA2S)₄-OMe; (b) synthetic decasaccharide (GlcNS6S-IdoA2S)₅-OMe.

heparin oligomers were chemically synthesized through an iterative oligomerization employing a GlcN-IdoA thioglycoside donor disaccharide bearing a GlcN-6-OBz protecting group.⁸ The oligosaccharides were of high chemical purity and were fully characterized by mass spectrometry, 800 MHz NMR, and PAGE to demonstrate comparability with digest length heparins.⁸

When these synthetic oligomers were used for experiments, adhesamine (1) exhibited the ΔH and ΔG values dependent on the length of the synthetic heparin oligomer, providing further support for our model (Supporting Information Figure S10). Molecule 7, which lacks one of the two pyrimidine rings, generated no detectable ΔH value (Supporting Information Figure S11). These results are consistent with those with the fractionated heparin oligomers and support our model of

cooperative association through pyrimidine–pyrimidine interactions.

We also noted that larger numbers of adhesamine bound to the fully sulfated synthetic heparin oligomers with larger ΔH values than to the fractionated ones (Table 1 and Supporting Information Figure S10c). The fractionated oligomers are mixtures of variably sulfated saccharides and generally less sulfated than the synthetic oligomers we used, suggesting the importance of sulfation levels for the interaction.

Selectivity of Adhesamine and Dimer-like Molecule 6.

Cooperative interactions have well been studied in DNA-binding peptide dimers. Covalently conjugated peptide dimers usually have higher affinity for DNA, but lower sequence selectivity, than naturally occurring non-covalent peptide dimers, suggesting that cooperative interaction plays a role in the finely tuned sequence recognition of DNA.⁹ Adhesamine, which discriminates heparan sulfate/heparin from other negatively charged glycosaminoglycans,¹ may achieve its selectivity by cooperative interaction with heparan sulfate/heparin. ITC experiments were conducted to compare the affinities of adhesamine and conjugate 6 for heparin vs chondroitin sulfate, another heavily sulfated glycosaminoglycan (Table 3 and Supporting Information Figure S12). We used

Table 3. Thermodynamic Values for the Interaction of 1 or 6 with Heparin or Chondroitin Sulfate A^a

	^{app} ΔH (kcal/mol)	^{app} ΔG (kcal/mol)	^{app} ΔS (cal/mol-deg)
1 + heparin	-219.4	-11.1	-699
1 + chondroitin sulfate A	nd	nd	nd
6 + heparin	-139.8	-12.0	-429
6 + chondroitin sulfate A	-91.7	-10.4	-272

^aAll data were collected in 50 mM sodium phosphate buffer (pH 6.0) containing 10 mM NaCl and 2% (v/v) DMSO at 25 °C. nd = not detectable, app = apparent values.

commercially available purified, fractionated heparin and chondroitin sulfate polymers of highest possible quality (average molecular weights: 15 kDa for heparin and 37.5 kDa for chondroitin sulfate). Adhesamine exhibited a strong affinity for heparin (apparent $\Delta G = -11.1$ kcal/mol), but no detectable affinity for chondroitin sulfate. Conjugate 6 displayed less selectivity, with apparent ΔG values of -12.0 and -10.4 kcal/mol for heparin and chondroitin sulfate, respectively. Cooperative association mediated by non-covalent interactions of adhesamine molecules might be important in achieving adhesamine's selectivity for heparan sulfate/heparin.

Heparin Assembly. ITC analysis of the affinity of adhesamine for heparin polymer showed an enthalpy change larger than the values anticipated from those for octa- and deca-saccharides (apparent $\Delta H = -220$ kcal/mol; Tables 1 and 3). Similar sharp increases in enthalpy changes have been observed in cases of large conformational changes¹⁰ or self-assemblies, and clustering of heparan sulfate-bound syndecans is known to be important for physiological cell attachment.¹¹ Therefore, we hypothesized that adhesamine induces clustering or assemblies of heparan sulfate/heparin. To confirm the adhesamine-induced assembly of heparin, dynamic light scattering (DLS) experiments were carried out.¹² The intensity correlation function of heparin was larger and decreased more slowly in the presence of adhesamine than in the absence of

adhesamine, whereas that of chondroitin sulfate was essentially unchanged in the presence of adhesamine (Supporting Information Figure S13). The calculated hydrodynamic radii of adhesamine–heparin clusters were ~ 100 times larger than the radii of the control samples (Figure 5). These results indicate that adhesamine induces assemblies of heparin but not of chondroitin sulfate A.

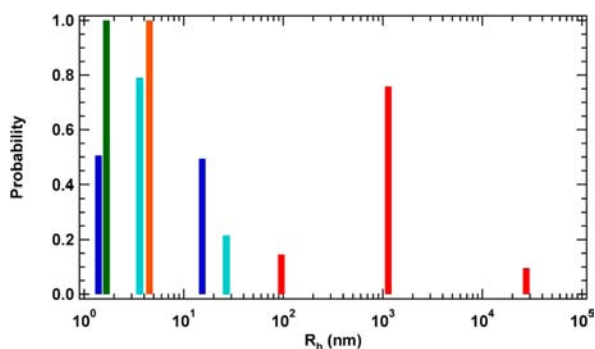


Figure 5. Heparin assembly observed by DLS. The size distribution functions were obtained utilizing manual fitting procedure for analysis of DLS results (Supporting Information Figure S13). R_h showed hydrodynamic radii. Individual tracings are (green) heparin ($4 \mu\text{M}$), (blue) chondroitin sulfate A ($20 \mu\text{M}$), (orange) adhesamine ($150 \mu\text{M}$), (red) heparin ($4 \mu\text{M}$) plus adhesamine ($150 \mu\text{M}$), and (cyan) chondroitin sulfate A ($20 \mu\text{M}$) plus adhesamine ($150 \mu\text{M}$).

Syndecans Clustering on the Cell Surface. Immunostaining experiments using mouse NIH3T3 cells were conducted to examine the ability of adhesamine to induce the clustering of the heparan sulfate-bound syndecans on the cell surface. We used fibronectin ($10 \mu\text{g}/\text{mL}$) as a positive control, which has been shown to induce cell spreading at this concentration.¹³ Similar to fibronectin, adhesamine induced large dots of syndecan-4, a heparan sulfate-bound syndecan that is known to be involved in cell attachment, whereas the control treatment with DMSO alone showed less clustering of syndecan-4 (Figure 6A, and its statistical analysis in Figure 6B). Physiological cell attachment by fibronectin or adhesamine was confirmed by observation of actin stress fiber formation (Figure 6A). In contrast to syndecan-4, adhesamine exhibited no statistically significant clustering of syndecan-1 or syndecan-2 (Supporting Information Figure S14). Immunostaining patterns of syndecan-3 were not clearly observed even with fibronectin, and syndecan-3 transcript was not detectable by RT-PCR.

To confirm the contribution of each syndecan, we performed siRNA knockdown experiments of syndecan-1, -2, and -4 by using a mixture of four siRNAs for each syndecan. Adhesamine induced clear cell spreading of the cells transfected with a negative control siRNA. In contrast, knockdown of syndecan-4 resulted in the most significant reduction of adhesamine-induced cell spreading among the syndecans we tested (Figure 7), while all the syndecans were knocked down equally well as judged by RT-PCR (Supporting Information Figure S15). The selectivity of the syndecan-4 knockdown was confirmed by using two other commercially available siRNAs for syndecan-4, which also reduced adhesamine-induced cell spreading (Supporting Information Figure S16). These results collectively suggest that syndecan-4 is essential in the adhesamine-induced cell adhesion.

Consistent with our results with adhesamine, clustering of syndecan-4 is known to play a pivotal role in cell adhesion.¹⁴

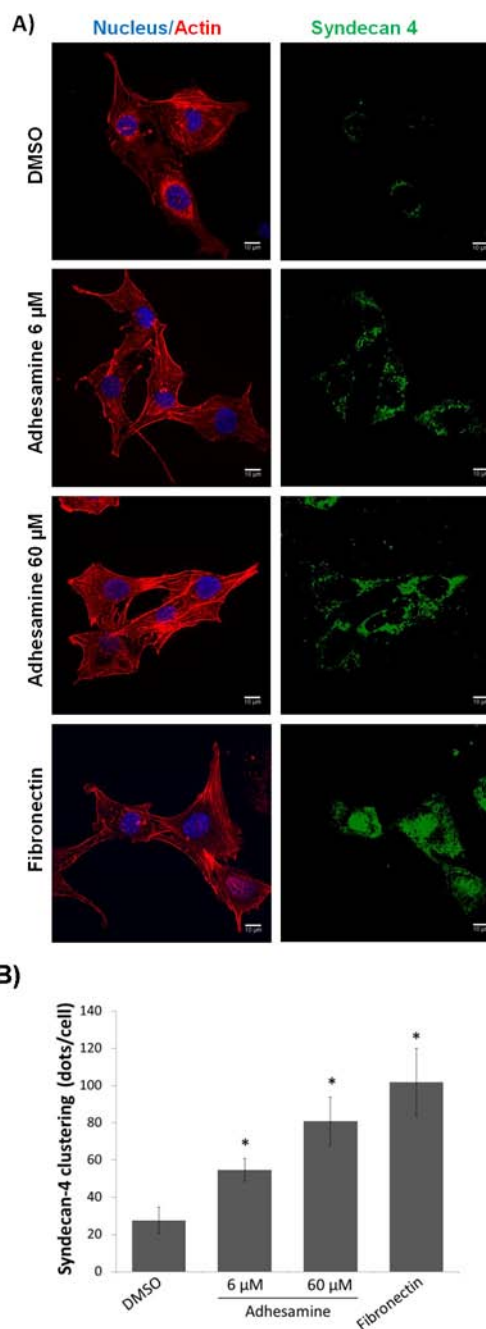


Figure 6. (A) Representative immunofluorescent images. NIH3T3 cells plated on glass plates were serum-starved for 24 h and then incubated with adhesamine (6 or $60 \mu\text{M}$), DMSO (1%), or fibronectin ($10 \mu\text{g}/\text{mL}$) for 2 h. After fixation with 4% paraformaldehyde, the cells were subjected to fluorescent staining with an anti-syndecan-4 antibody (5G9), DAPI (nucleus), and rhodamine phalloidin (actin stress fiber). Scale bar = $10 \mu\text{m}$. (B) Quantification of syndecan-4 clustering. Using Image-J Software, an individual cell was analyzed by counting the number of green dots which represent syndecan-4 clustering. Clustering data were pooled from three independent experiments. $*P < 0.05$ compared with the control group ($n = 9$ cells).

Syndecan-4 is associated with focal adhesions that form on substrates of fibronectin, laminin, vitronectin, or type I collagen.¹⁵ Overexpression of syndecan-4 leads to enhanced focal adhesion assembly and reduced cell motility, whereas syndecan-4 mutants show reduced focal adhesion assembly and cell spreading.¹⁶

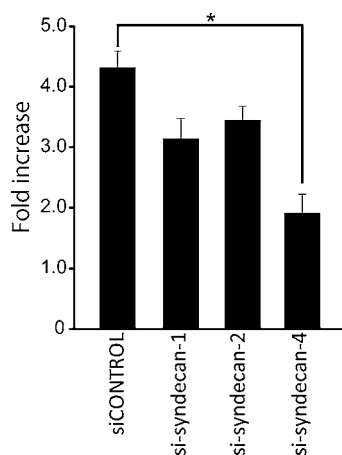


Figure 7. Effect of syndecan knockdown on adhesamine-enhanced cell spreading. NIH3T3 cells were transfected with siRNA for syndecan-1, -2, or -4, and incubated for further 2 days. The cells were cultured for 1 h on 96-well plates with DMSO (1%) or adhesamine (60 μ M). The number of round and spread cells was counted and normalized to that of DMSO. The values represent the mean \pm SE. * P < 0.05 compared with the control (n = 6).

Pilot Studies *in Vivo*. Extracellular matrix-induced clustering of heparan sulfate-bound syndecans is known to be an important driving force for cell adhesion and cell viability.¹¹ The ability of adhesamine to induce assembly of heparin *in vitro* and clustering of heparan sulfate-bound syndecans in cell culture prompted us to examine the extracellular matrix-like effects of adhesamine in living animals. Controlled incorporation of transplanted cells in host tissues and organs is a major challenge in cell therapy or in generating disease models, and co-injection of extracellular matrix is known to promote engraftment of cells injected in living animals.^{17,18} We conducted pilot animal studies (Figure 8) in which luciferase-labeled NIH3T3 cells¹⁹ were injected subcutaneously into skin wounds in mice, with or without adhesamine. In the absence of adhesamine, the transplanted cells declined to an undetectable

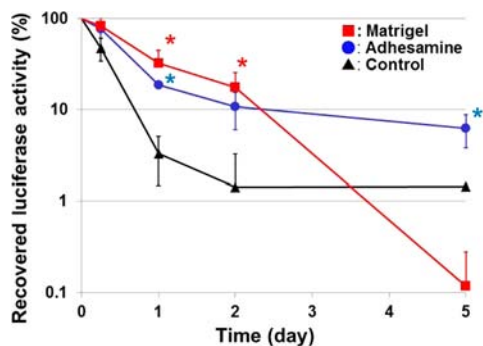


Figure 8. Effects of adhesamine on survival of transplanted cells. NIH3T3/Luc cells (5×10^5 cells) were subcutaneously injected into 8-mm full-thickness excisional skin wound in mouse models. Luciferase assays were performed at each indicated time. Individual tracings are (red squares) with Matrigel (50 μ L of a 10 mg/mL solution), (blue circles) with adhesamine and (black triangles) without adhesamine (50 μ L of a 50 μ g/mL [\sim 60 μ M] solution). Differences among the three groups were statistically evaluated by one-way ANOVA followed by Fisher's PLSD test. Adhesamine improved cell survival and resulted in statistically higher survival than the control on days 1 and 5. * P < 0.05 compared with the control group (n = 3 or 5).

level 2 d after transplantation. In contrast, co-injection with adhesamine (50 μ g/mL [\sim 60 μ M]) promoted viability, at comparable levels to those of Matrigel (10 mg/mL), a solubilized basement membrane from mouse sarcoma which has well been known to support cell survival of grafted cells *in vivo* animal models at this concentration.¹⁷

We also examined if adhesamine is useful in generating mouse xenografts of human cancer cells. Luciferase-labeled B16-BL6 melanoma cells were injected into mice from the tails, and luciferase activities in lungs were measured (Figure 9). Co-

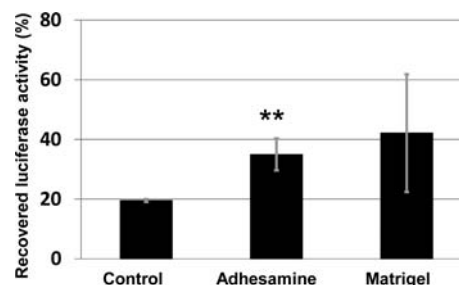


Figure 9. The effects of adhesamine on the lung metastasis. Luciferase-labeled B16-BL6 melanoma cells were injected from mouse tails together with adhesamine (50 μ L of a 50 μ g/mL [\sim 60 μ M] solution) or Matrigel (50 μ L of a 10 mg/mL solution). The attachment of B16-BL6/Luc cells in mouse lungs was estimated by measuring the luciferase activity in the lung tissue homogenates 2 h after inoculation of B16-BL6/Luc cells into the tail vein. ** P < 0.01 compared with the control group (n = 3).

injection of adhesamine (50 μ g/mL [\sim 60 μ M]) increased lung metastasis 1.8 \pm 0.25 folds, just as co-injection of Matrigel (10 mg/mL), which has previously been used for xenotransplant models.¹⁸

These results demonstrate that the non-peptidic, chemically defined small molecule improved survival of the grafted cells as much as Matrigel, an undefined mixture of proteins and growth factors. Matrigel's gelatinous physical properties are thought to resemble the extracellular environment that promotes survival of suspended cells. Further investigation is needed for understanding whether and how adhesamine mimics such environment. The ability of adhesamine to induce cell-surface assemblies might provide one possible explanation. Although the utility of adhesamine and its analogues requires validation and optimization through further animal studies, the present results provide a step forward in the application of these small molecules in cell therapy.

CONCLUSION

In conclusion, results of the present study suggest that adhesamine binds cooperatively and selectively to cell-surface heparan sulfate, induces clustering of syndecan-4, and thereby promotes physiological cell adhesion. It remains unclear how the interaction of adhesamine induces clustering of heparin sulfate/syndecans. Presumably, newly generated surfaces of heparan sulfate upon interactions with multiple adhesamine molecules drive the formation of mesoscale assemblies. Self-assembly of small molecules (aggregators) is increasingly observed in drug screening,²⁰ and our study provides another important example of such bioactive molecules. Increasing evidence also suggests that cell-surface heparan sulfate is important for the attachment and differentiation of clinically important cells, including human ES cells and iPS cells.²¹ The

results of the present study might provide a basis for the design of assembly-inducing small molecules that are useful for biological and medical applications.

EXPERIMENTAL SECTION

Isothermal Titration Calorimetry (ITC). ITC experiments were performed at 25 °C using a MicoCal iTC200 microcalorimeter. Adhesamine and its analogues were titrated with 17 × 2 μL injections of glycosaminoglycans (1 mM of heparin oligosaccharides, 25 or 50 μM of heparin, 100 μM of chondroitin sulfate A). The concentrations of adhesamine and its analogues are measured by HPLC (peak area at 254 nm). The titrations were performed in a 50 mM phosphate buffer (pH 6.0) containing 10 mM NaCl and 2% (v/v) DMSO. The raw data of these titrations are provided in Supporting Information.

Dynamic Light Scattering (DLS). DLS measurements were performed on a DLS standard setup with He–Ne laser ($\lambda = 632.8$ nm) and an Avalanche Photo Diode (APD, ALV, Langen, Germany) mounted on a CGS-5022F goniometer with an ALV-5000/EPP multi-tau digital correlator (both ALV, Germany). Reactant solutions were filtered (0.45 μm; Pall Corporation) prior to mixing and were transferred to the cylindrical cuvettes with the diameter of 10 mm after the mixing for 30 min. All the measurements were performed at 25 °C under a temperature controlled environment, and the scattering angle was fixed at 90°. The sample buffer used is 50 mM phosphate buffer (pH 6.0) containing 10 mM NaCl and 2% (v/v) DMSO.

Visualization of Syndecans-1, -2, and -4. 96-well glass bottom black microtiter plates (Greiner Bio One) were used for immunostaining of syndecans. A 100 μL NIH3T3 cell suspension in serum-free culture medium (DMEM, Gibco) was added to each well (5×10^3 cells/well). After incubation for 24 h, the following compounds were added to each well: adhesamine (6 or 60 μM), fibronectin (10 μg/mL), and DMSO (1%). A 60 μM dose of adhesamine exhibited higher activity than a 6 μM dose with NIH3T3 cells under the conditions we used. We therefore used the 6 or 60 μM doses throughout the present studies. After a 2-h incubation at 37 °C, non-adhered cells were removed by washing once with PBS. The cells were fixed for 15 min at room temperature with 4% (w/v) paraformaldehyde, permeabilized with 0.2% (w/v) Triton X-100 in PBS for 5 min, and then blocked with 5% BSA in PBS overnight at 4 °C. The cells were then treated with anti-syndecan antibodies in the blocking solution for 1 h, followed by PBS wash and treatment with Alexa Fluor 488-conjugated goat anti-rabbit IgG or Alexa Fluor 488-conjugated goat anti-mouse IgG, in the blocking solution for 1 h. The cells were washed three times with PBS after each step. The cells were also co-stained with DAPI and rhodamine phalloidin to visualize the nucleus and actin stress fiber, respectively. The cells were observed in PBS buffer containing 50% (w/v) glycerol. The confocal images of the cells were captured with a Cell Voyager CV1000 (Yokogawa Electric Corp.) with laser excitation at 561 nm for actin stress fiber, 488 nm for syndecan, and 405 nm for nucleus. The data were analyzed by using an Image-J Software (National Institutes of Health). The numbers of clustering syndecans per cell were counted and statistically analyzed. Student's *t* test was used to examine the difference between the negative control and the treatment groups. The results represent the means ± SD (*n* = 9 cells). Three independent experiments were performed for validation. More detailed procedure of quantification of the syndecan clustering is provided in the Supporting Information.

Animal Studies. Male ICR mice (5- or 15-week-old) and male C57BL/6 mice (5-week-old) were maintained on standard food and water under conventional housing conditions. The protocols for animal experiments were approved by the Animal Experimentation Committee of Graduate School of Pharmaceutical Sciences of Kyoto University. Detailed animal experiments are described in the Supporting Information.

ASSOCIATED CONTENT

Supporting Information

Gradient native polyacrylamide gel images, adhesion-promoting activities, representative ITC titration data, CD spectra, immunofluorescent images and statistical analysis of syndecans, knockdown of syndecan, characterization data, including ¹H NMR spectra, for all new compounds; procedures for X-ray crystallographic analysis, chemical synthesis of adhesamine analogues, cell adhesion assays, CD spectroscopy, and animal experiments. This material is available free of charge via the Internet at <http://pubs.acs.org>.

AUTHOR INFORMATION

Corresponding Author

uesugi@scl.kyoto-u.ac.jp; makiya@pharm.kyoto-u.ac.jp

Notes

The authors declare no competing financial interest.

ACKNOWLEDGMENTS

This work was supported by JST (AS2111048G), JSPS (LR018), ZE Research Program, IAE (B-10), and MRC Grant G902173. We also thank T. Morii and E. Nakata for sharing their equipment and experimental support. The Uesugi, Tokitoh, and Kanaya research groups participate in the Global COE program "Integrated Materials Science" (#B-09). iCeMS is supported by World Premier International Research Center Initiative (WPI), MEXT, Japan.

REFERENCES

- (1) Yamazoe, S.; Shimogawa, H.; Sato, S.; Esko, J. D.; Uesugi, M. *Chem. Biol.* **2009**, *16*, 773.
- (2) Hoshino, M.; Tsujimoto, T.; Yamazoe, S.; Uesugi, M.; Terada, S. *Biochem. J.* **2010**, *427*, 297.
- (3) (a) Schuksz, M.; Fuster, M. M.; Brown, J. R.; Crawford, B. E.; Ditto, D. P.; Lawrence, R.; Glass, C. A.; Wang, L. C.; Tor, Y.; Esko, J. D. *Proc. Natl. Acad. Sci. U.S.A.* **2008**, *105*, 13075. (b) Saito, Y.; Imazeki, H.; Miura, S.; Yoshimura, T.; Okutsu, H.; Harada, Y.; Ohwaki, T.; Nagao, O.; Kamiya, S.; Hayashi, R.; Kodama, H.; Handa, H.; Yoshida, T.; Fukai, F. *J. Biol. Chem.* **2007**, *282*, 34929. (c) Araki, E.; Momota, Y.; Togo, T.; Tanioka, M.; Hozumi, K.; Nomizu, M.; Miyachi, Y.; Utani, A. *Mol. Biol. Cell* **2009**, *20*, 3012. (d) Rodrigo, A. C.; Barnard, A.; Cooper, J.; Smith, D. K. *Angew. Chem., Int. Ed.* **2011**, *50*, 4675. (e) Choi, S.; Clements, D. J.; Pophristic, V.; Ivanov, I.; Vemparala, S.; Bennett, J. S.; Klein, M. L.; Winkler, J. D.; DeGrado, W. E. *Angew. Chem., Int. Ed.* **2005**, *44*, 6685. (f) Szelke, H.; Harenberg, J.; Kramer, R. *Thromb. Haemost.* **2009**, *102*, 859. (g) Liu, S. C.; Zhou, F. Y.; Hook, M.; Carson, D. D. *Proc. Natl. Acad. Sci. U.S.A.* **1997**, *94*, 1739. (h) Tashiro, K.; Nagata, I.; Yamashita, N.; Okazaki, K.; Ogomori, K.; Tashiro, N.; Anai, M. *Biochem. J.* **1994**, *302*, 73. (i) Woods, A.; McCarthy, J. B.; Furcht, L. T.; Couchman, J. R. *Mol. Biol. Cell* **1993**, *4*, 605. (j) Charonis, A. S.; Skubitz, A. P. N.; Koliakos, G. G.; Reger, L. A.; Dege, J.; Vogel, A. M.; Wohlhueter, R.; Furcht, L. T. *J. Cell. Biol.* **1988**, *107*, 1253. (k) McAllister, R. E. *Thromb. Res.* **2010**, *125*, S162. (l) Tabor, C. W.; Rosenthal, S. M. *J. Pharmacol. Exp. Ther.* **1956**, *116*, 139. (m) Selinka, H.; Florin, L.; Patel, H. D.; Freitag, K.; Schmidtke, M.; Makarov, V. A.; Sapp, M. *J. Virol.* **2007**, *81*, 10970. (4) (a) Buczek, P.; Horvath, M. P. *J. Biol. Chem.* **2006**, *281*, 40124. (b) Brown, A. *Int. J. Mol. Sci.* **2009**, *10*, 3457. (c) Pabo, C. O.; Sauer, R. T. *Annu. Rev. Biochem.* **1992**, *61*, 1053. (d) Harrison, S. C.; Aggarwal, A. K. *Annu. Rev. Biochem.* **1990**, *59*, 933. (5) Edink, E.; Jansen, C.; Leurs, R.; Esch, I. J. P. D. *Drug. Discov. Today Tech.* **2010**, *7*, e189. (6) (a) Dunitz, J. T. *Chem. Biol.* **1995**, *2*, 709. (b) Whitesides, G. M.; Krishnamurthy, V. M. *Q. Rev. Biophys.* **2005**, *38*, 385.

- (7) (a) Fischer, J.; Hein, L.; Lullmann-Rauch, R.; vonWitzendorff, B. *Biochem. J.* **1996**, *315*, 369. (b) Chakrabarti, B.; Balazs, E. A. *Biochem. Bioph. Res. Commun.* **1973**, *52*, 1170. (c) Chung, M. C. M.; Ellerton, N. F. *Biopolymers* **1976**, *15*, 1409. (d) Salter, M. K.; Rippon, W. B.; Abrahamson, E. W. *Biopolymers* **1976**, *15*, 1213. (e) Salter, M. K.; Abrahamson, E. W.; Rippon, W. B. *Biopolymers* **1976**, *15*, 1251.
- (8) Miller, G. J.; Hansen, S. U.; Avizienyte, E.; Rushton, G.; Cole, C.; Jayson, G. C.; Gardiner, J. M. *Chem. Sci.* **2013**, *4*, 3218.
- (9) (a) Vinson, C. R.; Sigler, P. B.; Mcknight, S. L. *Science* **1989**, *246*, 911. (b) Talanian, R. V.; Mcknight, C. J.; Kim, P. S. *Science* **1990**, *249*, 769. (c) Cuenoud, B.; Schepartz, A. *Science* **1993**, *259*, 510. (d) Palmer, C. R.; Sloan, L. S.; Adrian, J. C.; Cuenoud, B.; Paoella, D. N.; Schepartz, A. *J. Am. Chem. Soc.* **1995**, *117*, 8899. (e) Morii, T.; Simomura, M.; Morimoto, S.; Saito, I. *J. Am. Chem. Soc.* **1993**, *115*, 1150. (f) Okagami, M.; Ueno, M.; Makino, K.; Shimomura, M.; Saito, I.; Morii, T.; Sugiura, Y. *Bioorg. Med. Chem.* **1995**, *3*, 777. (g) Morii, T.; Saimei, Y.; Okagami, M.; Makino, K.; Sugiura, Y. *J. Am. Chem. Soc.* **1997**, *119*, 3649. (h) Morii, T.; Yamane, J.; Aizawa, Y.; Makino, K.; Sugiura, Y. *J. Am. Chem. Soc.* **1996**, *118*, 10011. (i) Aizawa, Y.; Sugiura, Y.; Morii, T. *Biochemistry* **1999**, *38*, 1626. (j) Sato, S.; Hagihara, M.; Sugimoto, K.; Morii, T. *Chem.—Eur. J.* **2002**, *8*, 5066.
- (10) Edink, E.; Rucktooa, P.; Retra, K.; Akdemir, A.; Nahar, T.; Zuiderveld, O.; van Elk, R.; Janssen, E.; van Nierop, P.; van Muijlwijk-Koezen, J.; Smit, A. B.; Sixma, T. K.; Leurs, R.; de Esch, I. J. P. *J. Am. Chem. Soc.* **2011**, *133*, 5363.
- (11) (a) Tkachenko, E.; Rhodes, J. M.; Simons, M. *Circ. Res.* **2005**, *96*, 488. (b) Dovas, A.; Yoneda, A.; Couchman, J. R. *J. Cell. Sci.* **2006**, *119*, 2837. (c) Yoneda, A.; Couchman, J. R. *Matrix Biol.* **2003**, *22*, 25. (d) Bartlett, A. H.; Hayashida, K.; Park, P. W. *Mol. Cells* **2007**, *24*, 153.
- (12) Ziegler, A.; Seelig, J. *Biophys. J.* **2008**, *94*, 2142.
- (13) (a) Corbett, S. A.; Wilson, C. L.; Schwarzbauer, J. E. *Blood* **1996**, *88*, 158. (b) Prokopi, M.; Pula, G.; Mayr, U.; Devue, C.; Gallagher, J.; Xiao, Q.; Boulanger, C. M.; Westwood, N.; Urbich, C.; Willeit, J.; Steiner, M.; Breuss, J.; Xu, Q.; Kiechl, S.; Mayr, M. *Blood* **2009**, *114*, 723. (c) Veevers-Lowe, J.; Ball, S. G.; Shuttleworth, A.; Kielty, C. M. *J. Cell. Sci.* **2011**, *124*, 1288.
- (14) (a) Woods, A.; Couchman, J. R. *Curr. Opin. Cell Biol.* **2001**, *13*, 578. (b) Woods, A. *J. Clin. Invest.* **2001**, *107*, 935. (c) Bass, M. D.; Humphries, M. J. *Biochem. J.* **2002**, *368*, 1. (d) Bellin, R. M.; Kubicek, J. D.; Frigault, M. J.; Kamien, A. J.; Steward, R. L., Jr.; Barnes, H. M.; DiGiacomo, M. B.; Duncan, L. J.; Edgerly, C. K.; Morse, E. M.; Park, C. Y.; Fredberg, J. J.; Cheng, C. M.; LeDuc, P. R. *Proc. Natl. Acad. Sci. U.S.A.* **2009**, *106*, 22102. (e) Oh, E. S.; Woods, A.; Couchman, J. R. *J. Biol. Chem.* **1997**, *272*, 11805. (f) Echtermeyer, F.; Baci, P. C.; Saoncella, S.; Ge, Y.; Goetinck, P. F. *J. Cell Sci.* **1999**, *112*, 3433. (g) Grootjans, J. J.; Reekmans, G.; Ceulemans, H.; David, G. *J. Biol. Chem.* **2000**, *275*, 19933. (h) Levy-Adam, F.; Feld, S.; Suss-Toby, E.; Vlodavsky, I.; Ihan, N. *Plos One* **2008**, *3*, e2319.
- (15) Woods, A.; Couchman, J. R. *Mol. Biol. Cell* **1994**, *5*, 183.
- (16) (a) Longley, R. L.; Woods, A.; Fleetwood, A.; Cowling, G. T.; Gallagher, J. T.; Couchman, J. R. *J. Cell Sci.* **1999**, *112*, 3421. (b) Horowitz, A.; Tkachenko, E.; Simons, M. *J. Cell Biol.* **2002**, *157*, 715.
- (17) Uemura, M.; Refaat, M. M.; Shinoyama, M.; Hayashi, H.; Hashimoto, N.; Takahashi, J. *J. Neurol. Res.* **2010**, *88*, 542.
- (18) Ohashi, K.; Marion, P. L.; Nakai, H.; Meuse, L.; Cullen, J. M.; Bordier, B. B.; Schwall, R.; Greenberg, H. B.; Glenn, J. S.; Kay, M. A. *Nat. Med.* **2000**, *6*, 327.
- (19) Nishikawa, M.; Yamauchi, M.; Morimoto, K.; Ishida, E.; Takakura, Y.; Hashida, M. *Gene Ther.* **2000**, *7*, 548.
- (20) (a) Takaoka, Y.; Sun, Y.; Tsukiji, S.; Hamachi, I. *Chem. Sci.* **2011**, *2*, 511. (b) Zorn, J. A.; Wille, H.; Wolan, D. W.; Wells, J. A. *J. Am. Chem. Soc.* **2011**, *133*, 19630. (c) Kato, M.; Han, T. W.; Xie, S.; Shi, K.; Du, X.; Wu, L. C.; Mirzaei, H.; Goldsmith, E. J.; Longgood, J.; Pei, J.; Grishin, N. V.; Frantz, D. E.; Schneider, J. W.; Chen, S.; Li, L.; Sawaya, M. R.; Eisenberg, D.; Tycko, R.; McKnight, S. L. *Cell* **2012**, *149*, 753.
- (21) (a) Lanner, F.; Lee, K. L.; Sohl, M.; Holmborn, K.; Yang, H.; Wilbertz, J.; Poellinger, L.; Rossant, J.; Farnebo, F. *Stem Cells* **2010**, *28*, 191. (b) Kraushaar, D. C.; Yamaguchi, Y.; Wang, L. C. *J. Biol. Chem.* **2010**, *285*, 5907. (c) Klim, J. R.; Li, L. Y.; Wrighton, P. J.; Piekarczyk, M. S.; Kiessling, L. L. *Nat. Methods* **2010**, *7*, 989.